

Crystal phases of a glass-forming Lennard-Jones mixture

Julián R. Fernández

Comisión Nacional de Energía Atómica, Avenida Libertador, 8250 Capital Federal, Buenos Aires, Argentina

Peter Harrowell*

School of Chemistry, University of Sydney, New South Wales 2006, Australia

(Received 30 September 2002; published 22 January 2003)

We compare the potential energy at zero temperature of a range of crystal structures for a glass-forming binary mixture of Lennard-Jones particles. The lowest-energy ordered state consists of coexisting phases of a single component face centered cubic structure and an equimolar cesium chloride structure. An infinite number of layered crystal structures are identified with energies close to this ground state. We demonstrate that the finite size increase of the energy of the coexisting crystal with incoherent interfaces is sufficient to destabilize this ordered phase in simulations of typical size. Two specific local coordination structures are identified as of possible structural significance in the amorphous state. We observe rapid crystal growth in the equimolar mixture.

DOI: 10.1103/PhysRevE.67.011403

PACS number(s): 61.43.Bn, 81.05.Kf, 61.43.Dg

I. INTRODUCTION

In this paper we examine the relative stability of a range of crystal phases of a model glass-forming liquid consisting of a binary Lennard-Jones mixture. There are a number of reasons why we are interested in identifying the stable crystal phases of glass-forming liquids. Here are six. (i) In order to determine the degree of supercooling of a mixture at a given composition we must first determine the equilibrium freezing point at that composition. This requires the identification of the crystal phase(s). (ii) Stable crystal structures identify stable local arrangements. While this by no means exhausts the local structural possibilities, these crystal coordinations are important candidates in any search for structures that stabilize the amorphous state [1]. (iii) To answer the question, why doesn't the supercooled mixture freeze, we need the relevant crystal structures to determine the probability of nucleation. (iv) Real glassy alloys do crystallize [2,3] and there are many questions of interest concerning crystal growth from the glass [2,4] that can only be addressed with explicit reference to the equilibrium crystal state. (v) The crystal phases represent lower bounds to the potential energy surface. If we add interphase regions, grain boundaries, and defects to these crystalline configurations, we have important contributions to the structure of the "low lands" of the potential energy landscape. Given the difficulty of accessing these low energy regions through molecular dynamics simulations of thermal quenches of the liquid, the crystal phase may provide a useful alternate "entry" point to these configurations. (vi) There are a variety of important nonequilibrium routes to glass formation, in particular high energy irradiation [5] and mechanical milling [6], which start from the equilibrium crystal state rather than the liquid.

There is a steadily growing number of model particles that are used in simulation studies of glassy behavior. These include molecular glass formers (e.g., propylene glycol [7],

orthoterphenyl [8], and the fluctuating bond model of a dense polymer [9]) and simple liquids with structural constraints (e.g., the Dzuganov icosahedral potential [10] and the Rome liquid [11]). Binary mixtures have been employed in modeling glass-forming alloys, using Lennard-Jones [12–14] or soft sphere potentials (in 3D [15–17] and 2D [18,19]), and ceramic glasses—SiO₂ [20], ZnCl₂ [21], and (moving on to ternary systems) alkali silicates [22,23]. This list is not intended to provide a complete account of glass-forming models but, simply, to underscore the wide variety of specific interactions and degrees of freedom that can give rise to glassy behavior.

Across the range of classes of glass formers, the relaxation kinetics exhibits sufficiently similar features to encourage belief in some sort of universality. No such comfort attends the consideration of the multiparticle configurations that give rise to this kinetics. We shall, therefore, focus our attention specifically on binary alloys in 3D. There has been a considerable effort in characterising glassy behavior in binary mixtures of spherical particles interacting via Lennard-Jones or repulsive r^{-12} potentials. In spite of this effort, information about the stable crystalline phases and the equilibrium transition temperatures of these systems is, at best, incomplete. Vlot *et al.* [24] have examined the *AB* crystal structures of a symmetric Lennard-Jones mixture in which the *AA* and *BB* interactions are identical. Defining $s = \sigma_{AB}/\sigma_{AA}$, where σ_{ij} determines the interaction length between species *i* and *j*, the following crystal structures are found to have the lowest free energy (out of the crystal phases considered) within the following ranges of *s*: CsCl for $0.8 < s < 0.95$, NaCl for $0.6 < s < 0.8$ and wurzite for $s < 0.6$. Middleton *et al.* [25] have reported on the stability of a number of *A₄B* crystals in the case of a Lennard-Jones mixture which we shall consider in detail below.

Extensive phase diagrams have been calculated for binary mixtures of hard spheres for a number of diameter ratios [26–29]. The following crystal structures have been considered: pure and randomly substituted fcc, AlB₂, NaCl, NiAs, AB₁₃ and CsCl. Glass-forming mixtures of soft spheres have

*Electronic address: peter@chem.usyd.edu.au

been studied with a radius ratio between 0.72 to 0.83. Over this range of size differences, the most stable of these crystalline states is coexisting pure fcc crystals. In light scattering studies of mixtures of hard-sphere colloidal suspensions with a size ratio of 0.72, Hunt *et al.* [30] report the appearance of single component face centred cubic (fcc) crystals at either end of the composition range. In the midcomposition range, the amorphous phase is found to be very stable. The difficulty in nucleating crystals that differ significantly in composition from the liquid has typically been attributed to slow kinetics associated with compositional fluctuations. Recently, however, Auer and Frenkel [31] have demonstrated that the crystal-liquid interfacial energy in a polydisperse hard-sphere mixture shows a significant increase with increasing supercooling. Within the standard nucleation theory, this result means that the rate of nucleation will decrease at large supercoolings, quite independent of the temperature dependence of the kinetic prefactor. This effect diminishes with decreasing polydispersity.

It would seem to be of considerable benefit to identify the stable crystal phases specific to a well characterized glass-forming mixture. To this end we report on the zero temperature potential energies of a wide range of crystal structures for a glass-forming Lennard-Jones mixture.

II. MODEL AND ALGORITHM

In this paper we have studied the binary mixture introduced by Kob and Andersen [12] (hereafter called KA) as a model glass-forming liquid. In the KA model, the species A and B have the same mass m and interact by means of Lennard-Jones potentials $V_{\alpha\beta} = 4\epsilon_{\alpha\beta}[(\sigma_{\alpha\beta}/r)^{12} - (\sigma_{\alpha\beta}/r)^6]$ with $\alpha, \beta = A, B$, and the set of parameters $\epsilon_{AA} = 1.0$, $\sigma_{AA} = 1.0$, $\epsilon_{AB} = 1.5$, $\sigma_{AB} = 0.8$, $\epsilon_{BB} = 0.5$, and $\sigma_{BB} = 0.88$. The parameters were chosen so that the pair potentials were similar to those proposed by Weber and Stillinger [32] in their model of the Ni-P mixtures (species A and B , here, respectively). The standard composition $A_{80}B_{20}$ at which the KA mixture has been studied corresponds to a eutectic in the actual Ni-P system [33] and, as the maximum depression of the freezing point, is generally regarded as an optimum composition for glass formation. We note that no eutectic points have been established for the KA model. The KA potential is a non-additive potential ($\sigma_{AB} < \sigma_{AA} + \sigma_{BB}/2$) where the high ϵ_{AB} and the small σ_{AB} values are supposed to reflect the strong metal-metalloid bond. Following Ref. [12], we truncate and shift the potential at a cutoff distance of $2.5\sigma_{\alpha\beta}$. Reduced units were adopted throughout this paper: the unit of length is σ_{AA} , the unit of energy ϵ_{AA} , and the unit of time $\tau = \sqrt{m\sigma_{AA}^2/\epsilon_{AA}}$.

Minimization of the potential energy was carried out using a conjugate gradient scheme in the space of particle coordinates and three unit cell vectors— \mathbf{a} , \mathbf{b} , and \mathbf{c} . When minimizing the potential energy at constant volume, \mathbf{a} , \mathbf{b} , and \mathbf{c} are held fixed. As reported below, energy minimization at constant volume can result in final configurations with a negative pressure. To avoid these tensioned states, we have carried out minimizations at a constant pressure. This was done by minimizing the enthalpy at $T=0$ and a pressure P ,

i.e., $H = E + PV$. The volume is a function of the cell vectors according to $V/N = \mathbf{a} \cdot (\mathbf{b} \times \mathbf{c})/n_{cell}$, where n_{cell} is the number of atoms per unit cell. Note that by including changes in the orientation of the unit vectors we test for shear stability. The molecular dynamics simulations used the Nosé-Poincaré-Andersen Hamiltonian [34,35], which allows a correct sampling from an isothermal-isobaric distribution. The equations of motion were integrated using a generalized leapfrog algorithm [35]. For all our simulations we used periodic boundary conditions and, due to the stability of the symplectic algorithm, a fairly large time step of $\Delta t = 0.01\tau$.

III. RESULTS

A. Crystal energies at zero temperature

We have calculated the potential energy of a number of crystal structures for the KA potential under the constraint of zero pressure and temperature. The resulting energy for each structure is presented in Table I.

We can organize the various crystal structures examined here into four groups based upon the motivation for their inclusion. The first group consists of the single component structures: face centered cubic (fcc), hexagonal close packed, and body centered cubic. The second group contains a number of common crystals found in binary alloys. The structures in this group are: CsCl, NiAs, Cu_3Au , NaCl, ZnS, AlB_2 , Al_3Ni_2 , CaF_2 , Co_2Al_9 , and WC. Readers are referred to Wells [36] for details of these crystal configurations.

The third group of crystals was inspired by the lowest energy structure presented by Middleton *et al.* [25] for the KA potential. This crystal has an A_4B composition and consists of a body centered tetragonal arrangement of A particles with every fifth (001) plane of A 's replaced by B 's. We report the energy (at $P=0$) for this structure, labeled $L[1,1.5]$ in Table I. The crystal can be described as alternating layers of AB (CsCl structure) and pure A (fcc). The interface (see Fig. 1) between these two phases exhibits a surprising coherency. As shown in Fig. 2, the two phases join at their mutual (001) planes. The (100) planes of the AB crystal, normal to the interfacial (001) plane, are rotated with respect to the A (fcc) lattice so that they lie parallel to the (110) planes of A phase.

We have generalized the A_4B structure of Ref. [25] by varying the spacing between the AB/A interfaces. As the thickness of both the AB and the A regions can be varied throughout a sample, these structures represent, in the thermodynamic limit, an infinite number of layering possibilities at a continuum of compositions. We shall indicate an ordered structure consisting of a periodic sequence $m \times AB$ layers and $n \times A$ layers as the $L[m, n]$ structure. [Note that an AB layer consists of two (001) planes. The same is true of an A layer.]

The final group of crystals consists of just two structures: Ni_3P and the Al_2Cu . These structures are depicted in Figs. 3 and 4, respectively. Coordinates for the experimentally determined structure of Ni_3P have been reported [37]. This crystal has been included in recognition that the Ni-P system provided the motivation for the original potential [32] on which Kob and Andersen based the choice of Lennard-Jones param-

TABLE I. Minimum energies of crystal structures at $T=0$ and $P=0$ for the two component Lennard-Jones system using the KA parameters. The following data are provided for each structure: mole fraction x_B of particle, structure name, space group, number of particles n_{cell} per unit cell, density, and potential energy per particle E/N .

x_B	Structure	Space group	n_{cell}	Density	E/N
0.0	hcp	$P6_3/mmc$	2	1.07	-7.47
	fcc	$Fm\bar{3}m$	4	1.08	-7.46
	bcc	$Im\bar{3}m$	2	1.05	-7.14
0.125	Co ₂ Al ₉ (unstable)	$P4$	16	1.07	-6.79
0.20	L[10,15]	$P4/mmm$	50	1.28	-8.20
	L[1,1.5]	$I4/mmm$	10	1.29	-8.12
0.25	Ni ₃ P	$I\bar{4}$	32	1.34	-8.14
	Cu ₃ Au (distorted)	$P4mm$	4	1.19	-6.65
	Cu ₃ Au (unstable)	$Pm\bar{3}m$	4	1.21	-6.61
0.333	Al ₂ Cu	$I4/mcm$	12	1.47	-8.71
	CaF ₂	$Fm\bar{3}m$	12	1.30	-7.45
	AlB ₂ (unstable)	$P6/mmm$	6	1.05	-4.61
0.4	L[20,5]	$P4/mmm$	50	1.58	-9.08
	Al ₃ Ni ₂	$P\bar{3}m1$	5	decays to L[2,0.5]	
0.5	CsCl	$Pm\bar{3}m$	2	1.79	-9.57
	WC	$P\bar{6}m2$	2	1.61	-8.43
	NiAs	$P6_3mc$	4	1.61	-8.42
	NaCl	$Fm\bar{3}m$	8	1.58	-8.24
	zinc blende	$F\bar{4}3m$	8	1.02	-4.74
	wurtzite	$P6_3mc$	4	decays to CsCl	
1.0	hcp	$P6_3/mmc$	2	1.57	-3.74
	fcc	$Fm\bar{3}m$	4	1.58	-3.73

eters [12]. The structure is also an example of an ordered structure based on a ninefold coordination around the B particle. The A particles about the B form a tricapped trigonal prism as shown in Fig. 3(a). The Al₂Cu crystal consists of aligned stacks of antiprisms (i.e., twisted cubes) [36] (see Fig. 4). This structure has been included here because the antiprism is singled out by Wells [36] as the lowest energy arrangement of eight particles about a central one when the interaction is a repulsive one, varying as r^{-n} .

The lowest energy state found in this work consists of coexisting A (fcc) and AB (CsCl structure) crystals as shown in Fig. 5. At the composition $A_{80}B_{20}$, the energy/particle of these coexisting crystals (neglecting the interfacial energy in the thermodynamic limit) is -8.31 , well below the analogous amorphous energy -7.72 [38] and the energy of the previously reported $L[1,1.5]$ structure, -8.12 . We can include the energy cost of a coherent interface between the AB (CsCl structure) and A (fcc) with reference to the $L[10,15]$ structure and find only a small increase in the energy. (We note, in passing, that Ni₃P is considerably less stable than the structures related to the AB (CsCl structure) phase. Here, the KA model differs significantly from the actual Ni-P system.)

With regard to the layered A/AB crystals, we can improve slightly upon the energy of the $L[1,1.5]$ structure [25]. Let us indicate the structure from Ref. [25] as $AAAAABAAAAAB$ where each letter refers to the species present in a single

(001) layer. The lower energy structure is $AAAAAABAB$ with an energy -8.17 as compared to -8.12 for the previous structure. The latter structure, $L[2,3]$, essentially represents the minimum number of A/AB interfaces. This criterion appears to identify the lowest energy layered crystal at all compositions.

The kinetics of crystallization may not always permit the formation of the coherent interface and so it is of interest to get some idea of the magnitude of the energy of an incoherent interface between the A and AB phases. A spherical inclusion of the AB crystal was surrounded by the crystalline A phase for system sizes ranging from $N=1534$ to $N=57291$. The size of the inclusion was chosen to ensure the overall composition to be very close to $A_{80}B_{20}$ and the crystal structures were chosen such that the pressure would be equal through the two-phase system at a density of $\rho=1.2$ in the thermodynamic limit. For all but the largest number of particles, we annealed the system at constant density for between 1000 to 330 τ at a constant temperature $T=0.3$, providing for only a modest relaxation of the interfacial structure before energy minimization.

We find a significant increase in the energy/particle as compared to the coherent case (see Table II). The large interfacial energy associated with this incoherent interface results in a substantial dependence of the energy/particle on the system size. For the smallest system with $N=1534$, the

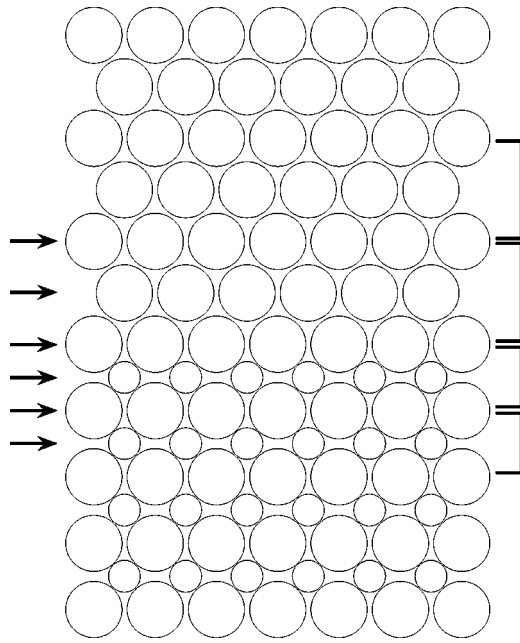


FIG. 1. Interfacial region in $L[10,15]$ structure optimized for the KA potential. The stacking of (001) planes on both pure A (fcc) and AB (CsCl), shown by the arrows, is similar to that found in the $L[1,1.5]$ structure of Middleton *et al.* [25]. Note the perfect coherency between the phases at the interface and the abrupt change in the layer width, indicated by the square brackets, in going from fcc to CsCl.

energy/particle of the two crystal phases is -7.81 , not far off that of the amorphous state for which $E/N = -7.72$. This result suggests that the amorphous state might be stabilized with respect to crystallization for small systems. This inversion of the relative stability of ordered and amorphous phases may be of interest with regards the formation of glasses by mechanical milling of crystalline material. While

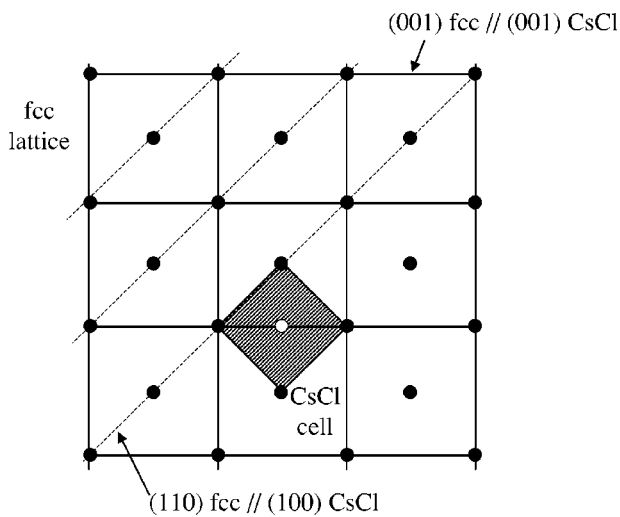


FIG. 2. Projection on the interfacial (001) plane showing the relative orientation of the fcc and the CsCl lattices in the coherent interface. The (100) planes of the AB (CsCl) crystal, normal to the interfacial (001) plane, are rotated so that they lie parallel to the (110) planes of the A (fcc) crystal.

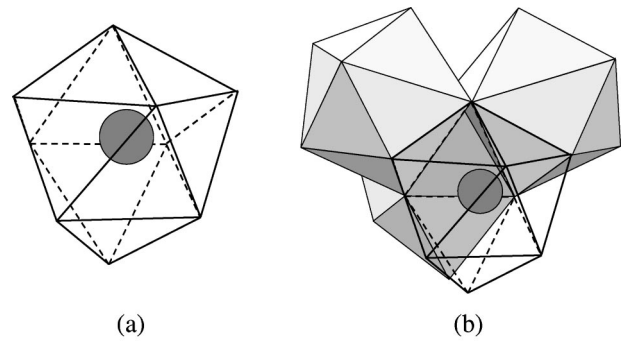


FIG. 3. Structure of the Ni_3P : (a) tricapped trigonal prism showing the ninefold coordination of A particles (at the vertices) around a B particle (central filled circle); (b) arrangement of these clusters in the Ni_3P structure sharing edges and triangular faces.

not claiming any physical significance of the particular interface modeled here, we do note that the fact that the ground state consists of coexisting phases naturally leads to the expectation of a system size dependence on the energy of that state.

Many of the simulations of the KA mixture at $A_{80}B_{20}$ have been carried out at a constant density, $\rho = 1.2$, rather than at a constant pressure. Under these conditions, we find the energy/particle of the coexisting $AB + A$ state (with the pressures of the two crystal phases equal) is -8.20 compared with the value of -7.72 for the $T=0$ amorphous state. At this density, the stable crystal coexistence is under tension with $P = -3.6$ at $T=0$. This implies that the energy of the ground state can be further reduced by introducing a vapor phase (at $T=0$ this will simply be a void). Doing so (and neglecting the interfacial contributions by invoking the thermodynamic limit) we find the energy/particle has decreased to -8.31 . We conclude that under the conditions of a density fixed at $\rho = 1.2$, the ground state of the $A_{80}B_{20}$ mixture is, in

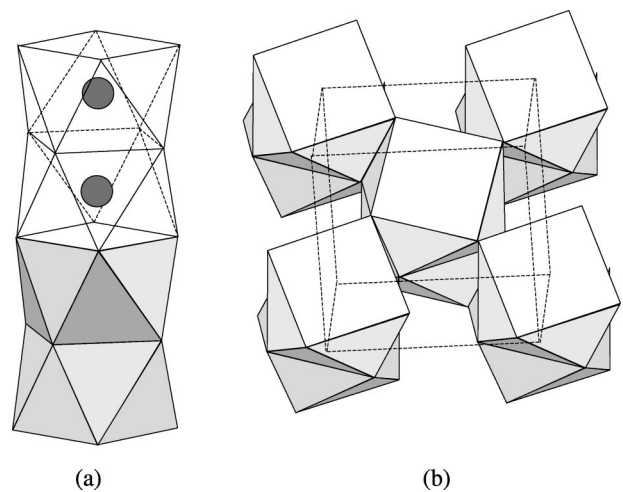


FIG. 4. Structure of the Al_2Cu : (a) antiprisms showing the eightfold coordination of A particles around a B particle, and their stacking in columns; (b) arrangement of these columns in the Al_2Cu structure sharing edges. The dashed lines show the tetragonal unit cell.

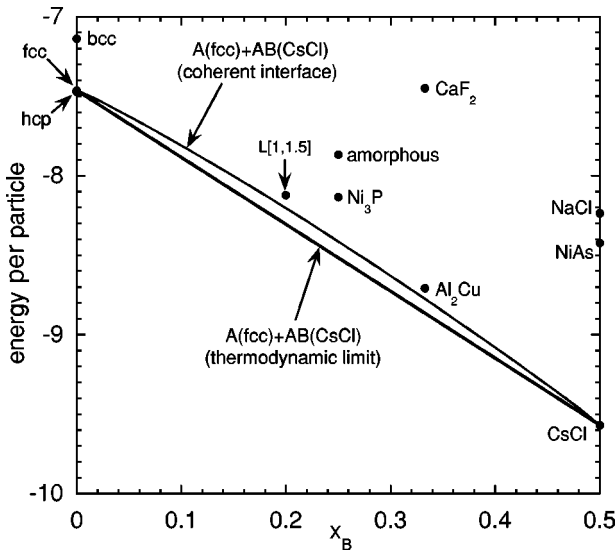


FIG. 5. Energy per particle (at $T=0$, $P=0$) vs composition of B , x_B , for the different structures studied in the KA model. The filled circles correspond to the structures of some common inorganic compounds. Note that for any composition the coexistence of A (fcc) and AB (CsCl) in the thermodynamic limit (straight line) is the energetically most favorable configuration. The curved line close to the thermodynamic limit indicates the energies for the coexistence of the same phases with a coherent (001) interface for the $L[m,n]$ structures (with $m+n=25$).

fact, quite complex: a three phase coexistence of vapor, A (fcc) and AB (CsCl structure).

B. Crystallization

We have carried out molecular dynamics (MD) runs on the equimolar KA mixture of $N=1458$ particles at fixed pressure ($P=0.0$) and temperature for a range of temperatures. We find that, on cooling, the mixture readily froze into the AB (CsCl structure) at $T=0.55$. The plot of the potential energy vs time in Fig. 6 is testimony to the rapidity of this transition. The resulting structure is highly ordered with a small number of point defects. This result confirms our identification of the AB crystal as the equilibrium ordered state in the $A_{50}B_{50}$ mixture.

TABLE II. The dependence of the energy per particle E/N and pressure P of a two-phase system of composition $x_B \approx 0.2$ on the total number of particles N . The A/AB interface is incoherent, constructed as described in the text at a density $\rho=1.2$. The initial configuration was relaxed via an MD run for the indicated time at $T=0.3$. This relaxation time was reduced with increasing system size due to CPU considerations. The $N=\infty$ data refer to the calculated energy in the thermodynamic limit as described in the text.

N	x_B	Relaxation time	P	E/N
1534	0.198	1000	-1.63	-7.81
3347	0.201	520	-2.32	-7.93
10063	0.200	330	-2.62	-7.99
57291	0.201	0	-2.94	-8.08
∞	0.20		-3.6	-8.20

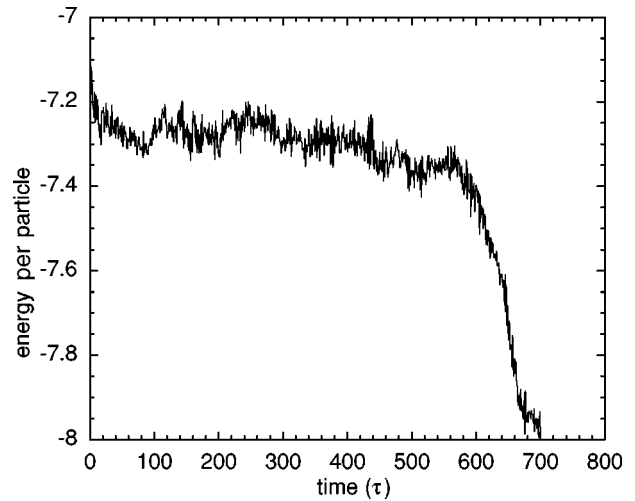


FIG. 6. The potential energy of the equimolar mixture at $P=0.0$ and $T=0.55$ as a function of time. Note the abrupt drop in potential energy associated with the transition to the crystalline state.

No crystalline ordering has ever been reported in the KA mixture at $A_{80}B_{20}$. In order to see if an order can be induced, we have seeded an $A_{80}B_{20}$ mixture of 8000 particles with an AB crystal seed of 91 particles. The seeded liquid was run for a period of 5650 τ at $P=0$ and $T=0.35$. At this temperature the average particle will have diffused a distance of 0.4 over the length of the run. The final configuration is shown in Fig. 7. We find that only 147 particles of the initially liquid particles (i.e., $\approx 2\%$) are found to be in a crystalline arrangement, almost all of them are A particles in an fcc arrangement.

Given the rapidity of crystallization in the equimolar mixture, it is unclear why crystal growth is not observed in the

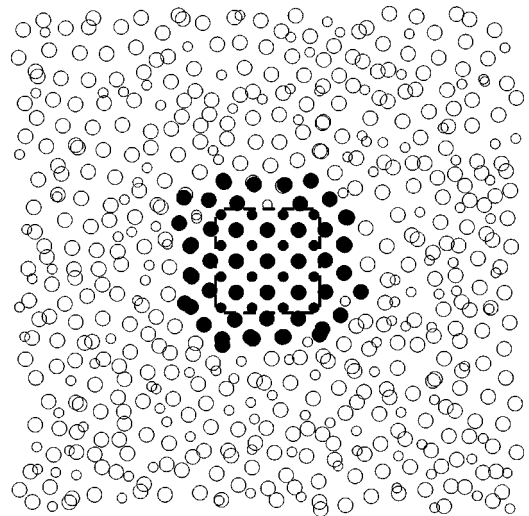


FIG. 7. Particle configuration for the $A_{80}B_{20}$ mixture ($N=8000$) with a rigid AB (CsCl) seed (dashed line) after a time $t=5650$ (at $T=0.35$ and $P=0$). Large (small) circles stand for A (B) particles, and filled (open) symbols indicate the particles in crystalline (noncrystalline) environments. Note that the crystalline particles around the seed consist of A particles in an fcc arrangement.

seeded $A_{80}B_{20}$ liquid. One possibility is that the freezing temperature has been significantly depressed at this composition with a resulting decrease in the chemical potential difference that drives the ordering. The magnitude of this freezing point depression has yet to be established. It is also possible that competition between the AB and A structures might conspire to frustrate growth. Both phases can be deposited at the (001) surface of either phase. The problem is that this deposited layers cannot contain both A and AB phases without high energy boundaries. As it was shown in Fig. 2, the deposited AB unit cell is rotated so that its (100) planes, perpendicular to the original surface, now lie parallel to the (110) planes of the fcc lattice. Attempting to accommodate both structures in a single plane would result in high energy grain boundaries and a destabilization of the growing crystal. The slow down of crystal growth by the conflict between incommensurate degenerate structures has been examined elsewhere [39].

IV. CONCLUSION

Following consideration of a number of crystal structures, we conclude that the equilibrium phase at $T=0$ for the binary Lennard-Jones mixture introduced in Ref. [12] consists of a coexistence between an AB (CsCl structure) crystal and a pure A (fcc) crystal with a coherent (001) interface. We also have identified a number of large unit cell structures with energies quite close to this ground state. These “structures of interest” include the A_2B (Al_2Cu structure) and the continuum of layered structures $L[m,n]$ and their random layered counterparts. The structural richness of these low energy configurations is in stark contrast to the idea that associates glass-forming ability with “frustration” of crystalline order. Free energy calculations are necessary to identify the equilibrium phases for $T>0$.

Our results are consistent with those of Vlot *et al.* [24] for the symmetric Lennard-Jones mixture. For the class of glass-forming mixtures with a dominant AB attraction, the interaction between the minority species (the BB interaction in this case) is of little consequence. One would expect little significant change, therefore, if the BB interaction is simply set equal to the AA interaction. This reasoning leads us to suggest that a symmetric Lennard-Jones mixtures should duplicate most of the behavior of the KA mixture while representing a parametrically simpler model for glass formation in this class of associating mixtures. Putting our results along side those from Ref. [24], it would appear that for models of associating mixtures consisting of Lennard-Jones particles with $\sigma_{AB}/\sigma_{AA} \geq 0.8$, the CsCl structure represents the only significant binary crystal. For size ratios below this value, rock salt and then the tetrahedral wurzite structure will dominate the phase diagram. It is of some interest to see if the differences between these ordered ground states are reflected in differences between the associated glassy states.

The identification of an inhomogeneous (i.e., coexisting) configurational ground state to this mixture means that the inevitable interfaces will contribute to the $T=0$ energy of any finite size sample. The combinatorics of the orientation and spatial distribution of these interfaces will, on its own,

result in a complex lower bound to the potential energy “landscape” over the space of particle configurations. The convergence of energy of the $A+AB$ phase with an incoherent phase boundary to that of the amorphous state is interesting. The amorphous state is likely to be stabilized with respect to crystallization in a sufficiently small system. The result also points to a spontaneous amorphization for a polycrystalline sample with domains below some critical size. While the coherent interface between the A and AB phases offers a much lower energy “option,” this applies only to the layered phase. Once we try to enclose one phase in another, the geometry of the geometrical restrictions of the coherent boundary require some high energy boundaries.

We have seen that the presence of a coherent interface between A (fcc) and AB (CsCl) does not significantly increase the energy. The resulting layered phases represent low energy ordered states at all compositions. This appears to preclude the possibility of a eutectic point within the composition range studied, unlike many real glass-forming alloys. This would mean that the stability of the amorphous phase owes little to freezing point suppression. It is possible, however, that the slow kinetics of layered growth might effectively negate their contribution.

We have identified two local eightfold coordinations of the small B particle by the A particles that represent structures of particular stability. These are the cube (as found in the CsCl structure) and the antiprism (as found in the Al_2Cu structure). The nine-particle tricapped trigonal prism (as found in the Ni_3P structure) appears as a stable structure with respect to the amorphous phase but not as stable as the 8-fold environments. While the naive polycrystalline models of the glass state have not stood up to detailed testing [40], there is a considerable literature on the connection between the medium range structure in amorphous solids and that in the relevant crystalline states [1]. The local structures identified here may play an important role in stabilizing the disordered solid. In slow quenches of the $A_{80}B_{20}$ KA mixture to $T=0$, over 90% of the B particles were found to be coordinated by either eight or nine A particles [41].

The failure of the $A_{80}B_{20}$ mixture to show any signs of ordering when seeded contrasts sharply with the rapidity of ordering in the $A_{50}B_{50}$ mixture. Understanding the stability of the former mixture captures the key challenge in the establishing principles that govern glass stability. We have suggested that crystallization may be frustrated due to the readiness with which A_8B clusters attach themselves to the (001) surfaces of the pure A domains. If something like this is responsible, then the kinetics of the local crystalline fluctuations may not only throw light on to the stability of the amorphous state with respect to freezing, but also on to the relaxation kinetics and thermodynamics of the amorphous state itself.

ACKNOWLEDGMENTS

We would like to acknowledge the support of the Australian Research Council and the Comisión Nacional de Energía Atómica of Argentina.

- [1] P.H. Gaskell, *Miner. Mag.* **64**, 425 (2000).
- [2] U. Köster and U. Herold, *Glassy Metals I*, Topics in Applied Physics Vol. 46, edited by H. Güntherodt and H. Beck (Springer-Verlag, Berlin, 1981), p. 225; A. Mashuhr, T. Waniuk, R. Busch, and W.L. Johnson, *Phys. Rev. Lett.* **82**, 2290 (1999); W. Liu, W.L. Johnson, S. Schneider, U. Geyer, and P. Thiyagarajan, *Phys. Rev. B* **59**, 11755 (1999).
- [3] P.N. Pusey and W. van Meegen, *Nature (London)* **320**, 340 (1986); *Phys. Rev. Lett.* **59**, 2083 (1987); S.I. Henderson and W. van Meegen, *ibid.* **80**, 877 (1998).
- [4] P. Harrowell and D. Oxtoby, *Ceram. Trans.* **30**, 35 (1993).
- [5] K. Samwer, H.J. Fecht, and W.L. Johnson, *Glassy Metals III*, Topics in Applied Physics Vol. 72, edited by H. Beck and H. Güntherodt (Springer-Verlag, Berlin, 1994), p. 5.
- [6] L. Schultz and J. Eckert, *Glassy Metals III*, Topics in Applied Physics Vol. 72, edited by H. Beck and H. Güntherodt (Springer-Verlag, Berlin, 1994), p. 69.
- [7] R. Leheny, N. Menon, S. Nagel, D. Price, K. Suzuya, and P. Thiyagarajan, *J. Chem. Phys.* **105**, 7783 (1996).
- [8] L.J. Lewis *Phys. Rev. B* **50**, 17 693 (1994).
- [9] K. Okun, M. Wolfgardt, J. Baschnagel, and K. Binder, *Macromolecules* **30**, 3075 (1997); J. Baschnagel, C. Bennemann, W. Paul, and K. Binder, *J. Phys.: Condens. Matter* **12**, 6365 (2000).
- [10] M. Dzugutov, *Phys. Rev. Lett.* **70**, 2924 (1993); J.P.K. Doye, D. Wales, F.H.M. Zetterling, and M. Dzugutov, e-print cond-mat/0205374 (2002).
- [11] R. Di Leonardo, L. Angelani, G. Parisi, and G. Ruocco, *Phys. Rev. Lett.* **84**, 6054 (2000); L. Angelani, R. Di Leonardo, G. Ruocco, A. Scale, and F. Sciortino, e-print cond-mat/0203301.
- [12] W. Kob and H.C. Andersen, *Phys. Rev. E* **51**, 4626 (1995).
- [13] S. Sastry, P. Debenedetti, and F.H. Stillinger, *Nature (London)* **393**, 554 (1998); S. Sastry, P. Debenedetti, F. Stillinger, T. Schroder, J. Dyre, and S. Glotzer, *Physica A* **270**, 301 (2002).
- [14] R. Della Valle, D. Gazzillo, and G. Pastore, *Mater. Sci. Eng., A* **165**, 183 (1993).
- [15] B. Bernu, J.P. Hansen, Y. Hiwatari, and G. Pastore, *Phys. Rev. A* **36**, 4891 (1987); T. Odagaki, J. Matsui, and Y. Hiwatari, *Phys. Rev. E* **49**, 3150 (1994).
- [16] R. Yamamoto and A. Onuki, *Phys. Rev. E* **58**, 3515 (1998).
- [17] H. Carruzzo and C. Yu, *Phys. Rev. E* **66**, 021204 (2002).
- [18] D. Deng, A. Argon, and S. Yip, *Philos. Trans. R. Soc. London, Ser. A* **329**, 549 (1989); 575 (1989); 595 (1989); 613 (1989).
- [19] D.N. Perera and P. Harrowell, *Phys. Rev. E* **59**, 5721 (1999).
- [20] R. Valle and H. Andersen, *J. Chem. Phys.* **97**, 2682 (1992); H. Schober and C. Oligschleger, *Phys. Rev. B* **53**, 11 469 (1996).
- [21] M. Wilson and P. Madden, *J. Phys.: Condens. Matter* **11**, A237 (1999).
- [22] J. Habasaki and Y. Hiwatari, *Phys. Rev. E* **65**, 021604 (2002).
- [23] R. Banhatti and A. Heuer, *Phys. Chem. Chem. Phys.* **3**, 5104 (2001); A. Heuer, M. Kunow, M. Vogel, and R. Banhatti, *ibid.* **4**, 3158 (2002).
- [24] M. Vlot, H. Huitema, A. de Vooy, and E. van der Eerden, *J. Chem. Phys.* **107**, 4345 (1997).
- [25] T.F. Middleton, J. Hernández-Rojas, P. N. Mortenson, and D.J. Wales, *Phys. Rev. B* **64**, 184201 (2001).
- [26] E. Trizac, M. Eldridge, and P.A. Madden, *Mol. Phys.* **90**, 675 (1997); M. Eldridge, P.A. Madden, and D. Frenkel, *ibid.* **80**, 987 (1993).
- [27] W. Kranendonk and D. Frenkel, *Mol. Phys.* **72**, 679 (1991).
- [28] D. Kofke and P. Bolhuis, *Phys. Rev. E* **59**, 618 (1999).
- [29] X. Cottin and P. Monson, *J. Chem. Phys.* **102**, 3354 (1995).
- [30] N. Hunt, R. Jardine, and P. Bartlett, *Phys. Rev. E* **62**, 900 (2000).
- [31] S. Auer and D. Frenkel, *Nature (London)* **413**, 711 (2001).
- [32] T.A. Weber and F.H. Stillinger, *Phys. Rev. B* **31**, 1954 (1985).
- [33] *Constitution of Binary Alloys*, 2nd ed., edited by M. Hansen and K. Anderko (McGraw-Hill, New York, 1958).
- [34] S.D. Bond, B.J. Leimkihler, and B.B. Laird, *J. Comput. Phys.* **151**, 114 (1999).
- [35] J.B. Sturgeon and B.B. Laird, *J. Chem. Phys.* **112**, 3474 (2000).
- [36] A.F. Wells, *Structural Inorganic Chemistry* (Clarendon Press, Oxford, 1975).
- [37] B. Aronsson, *Acta Chem. Scand.* (1947-1973) **9**, 137 (1955).
- [38] This value of the amorphous state energy at $T=0$ comes from the constant density calculations of Middleton *et al.* [25]. No value of the pressure was provided. Sastry *et al.* [42] noted that the pressure of the amorphous state for the KA potential at the same density becomes negative at a temperature below 0.06. We have therefore compared this energy with our own zero pressure calculations in the belief that it is at a pressure close to zero.
- [39] R. Khanna and P. Harrowell, *Phys. Rev. E* **56**, 1910 (1997).
- [40] G.S. Cargill, *J. Appl. Phys.* **41**, 12 (1970).
- [41] K. Vollmayr, W. Kob, and K. Binder, *J. Chem. Phys.* **105**, 4714 (1996).
- [42] S. Sastry, P.G. Debenedetti, and F.H. Stillinger, *Nature (London)* **393**, 554 (1998).